Insights into ligand stimulation effects on gastro-intestinal stromal tumors signalling

Christelle Bahlawane [a,*], Martine Schmitz [a], Elisabeth Letellier [a], Karthik Arumugam [b], Nathalie Nicot [c], Petr V. Nazarov [c], Serge Haan [a]

[a] Molecular Disease Mechanisms group, Life Sciences Research Unit, University of Luxembourg, Campus Belval, 6 Avenue du Swing, L-4367 Belvaux, Luxembourg
[b] Department of Infection and Immunity, LIH, 84 Val Fleuri, L-1526, Luxembourg
[c] Genomics Research Unit, LIH, 84 Val Fleuri, L-1526, Luxembourg

ABSTRACT

Mutations in KIT or PDGFRA are responsible for >85% of gastrointestinal stromal tumors. The introduction of imatinib in the GIST therapy scheme revolutionized the patient outcome. Unfortunately, the therapy allows the disease stabilization instead of curation. Furthermore the resistance to the inhibitor arises in most cases within two first years of therapy. A thorough investigation of the signalling pathways activated by the major PDGFRA and KIT mutants encountered in the GIST landscape allowed to identify striking differences between the two receptor tyrosine kinases. PDGFRA mutants were not responsive to their ligand, PDGFAA, and displayed a high constitutive kinase activity. In contrast, all KIT mutants retained, in addition to their constitutive activation, the ability to be stimulated by their ligand. Kit mutants displayed a lower intrinsic kinase activity relative to PDGFRA mutants, while the KIT Exon 11 deletion mutant exhibited the highest intrinsic kinase activity among KIT mutants. At the transcriptomic level, the MAPK pathway was established as the most prominent activated pathway, which is commonly up-regulated by all PDGFRA and KIT mutants. Inhibition of this pathway, using the MEK inhibitor PD0325901, reduced the proliferation of GIST primary cells at nanomolar concentrations. Altogether, our data demonstrate the high value of MEK inhibitors for combination therapy in GIST treatment and more importantly the interest of evaluating the SCF expression profile in GIST patients presenting KIT mutations.

1. Introduction

Gastro-intestinal stromal tumors (GIST) represent the most common mesenchymal neoplasm of the gastrointestinal tract. They arise from the interstitial cells of Cajal and are found essentially in the stomach (60% of the cases), in the small intestine (25%) but also in rectum, oesophagus and other locations outside the gut wall [1]. GIST are mainly due to mutations in KIT (75–85%) [1] or PDGFRA (10%) genes [2]. KIT and PDGFRA are type III receptor tyrosine kinases (RTKs), composed of three regions: (i) an extracellular domain responsible for ligand binding; (ii) a single transmembrane region with a juxtamembrane (JM) domain responsible for the kinase auto-inhibition properties; and (iii) a cytoplasmic domain that carries the kinase activity [3,4]. In the non-activated configuration, the JM domain blocks the kinase in a closed conformation impeding ATP molecules to access the catalytic site. After ligand binding, the wild type (WT) receptor dimerizes and tyrosine residues within the juxtamembrane domain are phosphorylated [3]. This induces conformational changes and releases the inhibitory function of this region towards the cytoplasmic domain [4]. Finally intermolecular phosphorylation at tyrosine residues serves as docking sites for SH2 domain containing molecules for further downstream signaling, which leads essentially to the activation of MAPK and PI3K pathways [4].

Mutations responsible for GIST occur mainly in the JM domain for KIT and in the kinase domain for PDGFRA, leading to constitutively activated receptors [2]. The nature of the mutation plays such an important role for the treatment schedule that the ESMO recommendations include a systematic molecular analysis in the diagnosis of GIST [5]. If surgery remains the treatment of choice for resectable tumors, adjuvant therapy is highly recommended for intermediate and high risk patients since >50% of patients relapse even after complete tumor resection [6]. In case of KIT Exon 9 or PDGFRA D842V mutations that confer resistance to imatinib, it is recommended either to start with high doses of imatinib or to switch to the second line therapy sunitinib [5]. Both drugs target the receptor tyrosine kinases themselves, competing with ATP for binding within the catalytic site. In addition to the primary resistance of certain types of mutations to imatinib, a appears frequently within the two first years of therapy as a result of the acquisition of secondary mutations within the kinase domain of the receptor [7]. Since the landscape

* Corresponding author.
E-mail address: christelle.bahlawane@uni.lu (C. Bahlawane).

of secondary mutations is quite broad within a single patient, the development of new generation of RTK inhibitors is not expected to cope with this issue. Therefore, the discovery of new targets for GIST therapy is essential. Hence we propose a thorough comparison of the signalling capacities, proffered by the main mutations found in GIST patients, in a homogenized background in order to identify common druggable targets.

2. Material and methods

2.1. Cell culture

The 293FR host cell line was generated from Hek293 cells by the co-transfection of the Flp-In™ target site vector (pFRT/lac Zeo, Invitrogen) and Tetracyclin repressor (pcDNA™6/TR, Invitrogen) as previously reported [8]. KIT mutant expressing cell lines were generated by the transfection of the Flp recombinase expression plasmid (pOG44, Invitrogen) together with the transgene expression plasmid (pcDNA5/FRT/TO-based, Invitrogen). Stably transfected cells were then selected and cultivated in the presence of 100 μg/ml Hygromycin and 10 μg/ml Blasticidin. Experiments were conducted under serum reduced (1%) conditions for 11 h and for additional 3 h under serum free (0% FBS) conditions using 5 ng/ml doxycycline (Sigma), unless differently stated in the figure legends. The stimulation of KIT and PDGFRA expressing cells was performed with SCF (100 ng/ml) and PDGF-AA (100 ng/ml), respectively (Immunotools).

GIST primary cell line GIST882 [9], presenting a homozygous missense mutation in KIT exon 13, and GIST48, a homozygous primary exon 11 missense mutation and a secondary heterozygous exon 17 missense mutation were generously provided by Dr. Sebastian Bauer (WTZ, Essen) and cultivated in RPMI and IMDM, respectively with 15% FBS in humidified atmosphere containing 5% CO_2. PD0325901 and XL-184 (Selleck Chemicals) were added to the medium 24 h after cell seeding for 30 h at the indicated concentrations. The stimulation of primary cell lines was performed after 6 h starvation to a final concentration of 100 ng/ml SCF. Cell viability was assessed with PrestoBlue (Thermofischer) in 96 well plate format following the manufacturer's recommendations. The fluorescence was monitored using the CLARIOstar microplate reader (BMG LABTECH).

2.2. Mutagenesis

KIT wild type cDNA was reverse transcribed from Mel501 RNAs (cells kindly provided by R. Halaban, [10]) and cloned into pCDNA5/FR/To plasmid after insertion of AscI and SgraI restriction sites by PCR. Plasmid was sequenced and compared to the c-KIT variant 2 mRNA sequence (NM_001093772.1). Two mutations were identified and fixed using Quik-change site-directed mutagenesis KIT (Stratagene) following the manufacturer's recommendations. The single point mutation V559D was prepared using the same procedure, while KIT Ex9 duplication mutant (AY502–503) and KIT Ex11 deletion mutant (553–557) were prepared by Life Technologies using GeneArt™Gene Synthesis. All plasmids were sequenced prior transfection to 293FR cells.

2.3. Flow cytometry analysis

Cell surface and total protein expression of KIT wild type and mutants were analyzed by flow cytometry using a FACS CantoII Instrument (Becton Dickinson, Heidelberg, Germany). 10^5 cells were harvested in the presence of PBS/10 mM EDTA and then washed with FACS-buffer (PBS/5%FCS/0.1%NaN3). Afterward, the cells were either directly incubated with 10 microL KIT primary antibody (anti-CD117-APC conjugated; C7244; Dako, Belgium) for cell surface expression, or first incubated with 0.1% saponin permeabilizing buffer prior KIT antibody incubation for total KIT expression. The specificity was controlled using an isotype-matched/ APC conjugated antibody (IgG1 kappa; ×0968, Dako, Belgium).

2.4. Model building and refinement with CHARMM

Since the kinase domain of KIT is located in the cytoplasmic region, the extracellular region was removed from the model building and the kinase insert region (residues 693 to 755) was replaced by Glycine residues. The initial models of KIT regions were built by homology modeling using MODELER9v7 on Linux based operating environment based on the crystal structures (PDB ID: 2EC8 and 2E9W) as templates. The primary 3-dimensional structure of KIT WT model was further improved by using energy minimization, followed by equilibration methods both in a vacuum and in an implicit membrane with implicit water solvation methods (EEF1) with CHARMM35 parameters. Finally, 20-ns molecular dynamics (MD) simulations were run with Langevin dynamics with a time step of 2 fs.

2.5. Western blot analysis

Cell lysis was performed on ice, using $1 \times$ Laemmli buffer. Proteins were subjected to SDS-PAGE, transferred to a polyvinylidene difluoride membrane (Roth) and then probed with the respective antibodies. The last are listed in the corresponding "Data in Brief article" [11]. Signals were detected on a Fusion-FX7 chemiluminescence detection device (Vilber) using a home-made ECL (Enhanced ChemiLuminescence) solution [12]. Signal intensities were quantified using the Bio1D analysis package (Vilber).

2.6. Microarray analysis

293FR cells expressing KIT-WT, KIT Ex11 deletion mutant and KIT Ex9 mutant were treated with 5 ng/ml doxycycline and 100 ng/ml SCF for 21 h in DMEM with 1%FCS. Cells were then starved for 3 h (without FCS) and further stimulated with SCF. Gene Expression analysis was performed using GeneChip Human Gene ST 2.0 arrays (Affymetrix). The raw data in the form of Affymetrix CEL files were imported into Partek® Genomics Suite™ software (Partek GS). The Robust Multichip Average (RMA) with GC correction was applied to the data set resulting in expression values for Affymetrix transcript clusters. Quality control and data normalization were performed as previously reported [13, 14]. We focused on differentially expressed genes (DEG) across the mutants comparing them with non-stimulated KIT-WT. To exclude non-relevant lowly expressed transcript clusters, only those showing $\log_2$ expression above 4.5 were considered for further analysis. Transcript clusters were further summarized in order to obtain a single expression value for each gene in each experiment. The differentially expressed genes were statistically evaluated by two-factor linear model with empirical Bayes statistical approach using *limma* package of R/Bioconductor [15]. In order to correct for the false discovery rate (FDR), the Benjamini & Hochberg step-up method correction was applied. Probe-sets with FDR <0.05 and absolute fold change >0.5 were considered to be significantly differentially expressed (DEGs). Microarray data are available in the ArrayExpress database (www.ebi.ac.uk/arrayexpress) under accession number E-MTAB-4548.

2.7. Rank-Rank analysis

In order to compare the different KIT mutants and wild-type signalling without any pre-defined cutoffs, we used the nonparametric rank-rank geometric overlap analysis (RRHO) [16] to identify the statistically significant overlap between the gene signatures. The probe sets were first ranked based on their signed log-transformed p-values of ANOVA results to compare between the subgroups and the control (non-stimulated wild-type KIT). The results of the analysis are represented as a group of two plots: 1. RRHO heat map. The heat map value, visualized

as pixel on the map. 2, represents the −log10 transformed hypergeometric *p*-value for the likelihood of presenting the observed degree of overlapped number of genes between both rank thresholds. The rank scatter plot represents the overlap between two signatures. Spearman rank correlation coefficient (rho) was calculated between the two compared gene signatures as previously done [8].

2.8. Quantitative PCRs

mRNAs for qPCRs were extracted, as for micro-array analysis, and used as templates for the cDNA synthesis with the high capacity cDNA reverse transcription KIT (Applied Biosystems) following the manufacturer's recommendation. Quantification was performed using ABsolute Blue QPCR SYBR Low ROX (Thermoscientific) on the AB7500 FAST PCR system (Applied Biosystems) following the MIQE guidelines [17]. Reference genes were selected using the Genorm software [18] included in the Qbase package (Biogazelle) used for the data analysis. Primers sequences are listed in Table 2 in [11].

3. Results

3.1. Selection of GIST mutations included in the present study

In the COSMIC database [19], about 3200 GIST samples are currently registered. KIT mutations represent 75%, PDGFRA 21% and WT 4% of all gastro-intestinal stromal tumors (Table 1), which is in line with large cohort studies previously published [1,20–22]. In this study we propose comparing the signalling features derived from the main KIT and PDGFRA mutations identified in GIST (Table 1). Therefore, we selected two types of mutation in KIT Exon 11, representing >62% of GIST, and one mutation in Exon 9, accounting for about 10% of GIST. Furthermore, two PDGFRA mutations (D842V and D842Y) within the kinase domain (15% of GIST) and one within the juxtamembrane domain (V561D) (3% of GIST) were included in the study. We took advantage of the recently implemented "in vitro" model where the above mentioned PDGFRA mutants were successfully investigated in an isogenic background [8]. We stably transfected Hek293/FR cells with different KIT constructs cloned in PCDNA5/To plasmid, namely KIT WT, KIT Ex9 (duplication AY 502–503), KIT V559D and KIT Ex11 del mutant (deletion of residues 553 to 557). PDGFRA mutants are included in this study for comparison purpose as they were deeply investigated previously [13].

3.2. KIT protein localization changes according to the mutation status

First, RNA and protein expression levels were assessed in the stably transfected cell lines. Adding doxycycline to the culture medium enhances KIT expression by a factor 100 and comparable mRNA expression levels were observed for all mutants (Fig. 1a in [11]). However, we could identify some differences in protein expression levels between KIT WT, KIT V559D and KIT Ex11, KIT Ex9 (Fig. 1b in [11]). Such a discrepancy between mRNA and protein expression levels was previously observed between wild type and PDGFRA mutants, and was linked to the protein activity [14]. Next we analyzed KIT surface expression for
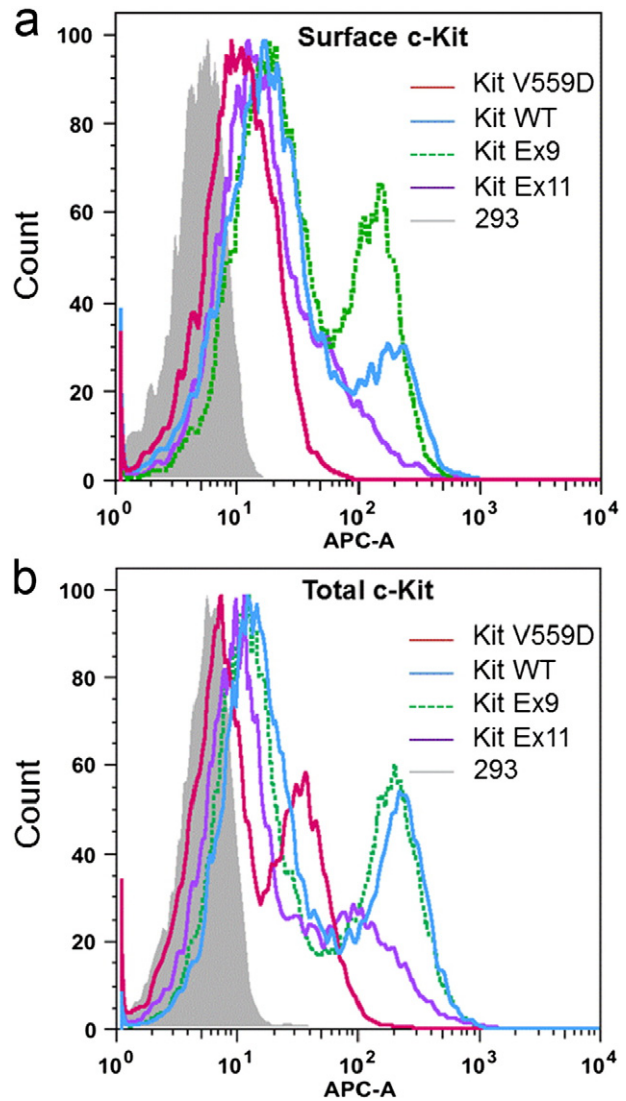
Fig. 1. KIT expression in the different KIT mutants. Protein expression was achieved by adding 5 ng/ml doxycycline to the medium for 14 h. **a.** Membrane KIT expression in KIT WT, KIT V559VD, KIT Ex9, KIT Ex11 was analyzed by flow cytometry. Histograms represent the number of cells as a function of the fluorescent intensity of KIT staining by an APC-conjugated anti-KIT antibody. **b.** Total KIT expression observed in KIT mutants (i.e., plasma membrane and intracellular staining). In both graphs, 293 non infected cells and isotype control staining were used as controls and are both represented by the gray solid histogram.

the different mutants by flow cytometry (Fig. 1a). KIT Ex9 mutant displayed the highest cell surface expression, followed by KIT WT, KIT Ex11 deletion mutant and KIT V559D. The ratio of surface (Fig. 1a) to total KIT expression (Fig. 1b) indicates the almost exclusive presence of KIT WT at the surface, while about 70% of KIT Ex9 is found at the

Table 1
Mutants investigated in this study with their incidence according to the COSMIC database.*

| Genes	Domains	Exon	Percentage in GIST patients according to the COSMIC database*	Mutations	Percentage of the investigated mutation among the mutations found within the exon
PDGFRA	Kinase	17	15.1	D842V	69.9
				D842Y	2.7
	Juxtamembrane	12	3.6	V561D	27.3
KIT	Juxtamembrane	11	62.8	V559X	13.1
				Del including res. 553–557	46.1
	Extra-cellular domain	9	9.6	Duplication 502–503 AY	86.1

* After removal of the unknown mutation (23% of all GIST present in the database, including WT).

surface. This value drops to 50% for both Ex11 mutants. After SCF addition, KIT surface expression decreases drastically for all KIT proteins (Fig. 2 in [11]). Furthermore, total protein expression decreased by >3.5 fold for the WT protein and by 1.5 vs. 1.2 fold for Ex9 and Ex11 mutants, respectively (Table 1 in [11]).

KIT occurs either as a complex glycosylated high molecular weight protein of 145 kDa (HMW), or as a high mannose decorated form with a lower molecular weight of 125 kDa (LMW) [23]. KIT WT is mainly expressed as HMW, which is a non-phosphorylated protein (Fig. 2a). Upon SCF addition, KIT is rapidly phosphorylated and subsequently

dephosphorylated and degraded (Figs. 1b and 3a in [11]). The JM domain mutants, KIT V559D (Fig. 2a) and KIT Ex11, are present in both HMW and LMW forms that are constitutively phosphorylated, while KIT Ex9 is present in both forms, where the HMW form is phosphorylated (Fig.2b).

In summary, contrasting protein expression is observed in stable cell lines expressing KIT WT or KIT mutants in the human Hek293 cells although they display similar KIT mRNA levels. KIT WT and KIT Ex9 display mainly HMW protein present at the cell surface, while KIT Ex11 displays mainly the LMW form, which is retained in the intracellular
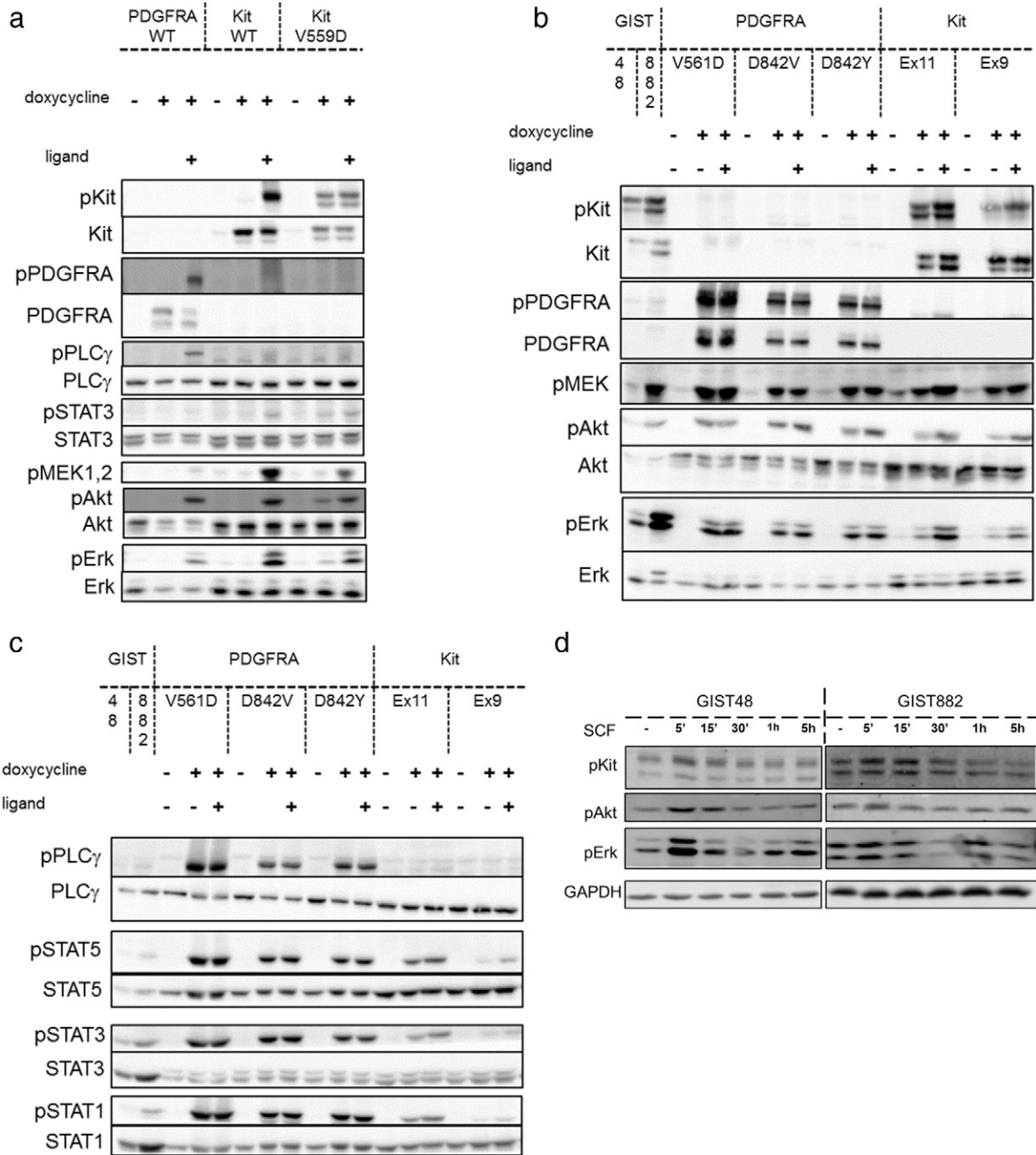
Fig. 2. Signalling capacities of GIST mutants compared to PDGFRA and KIT WT signalling. Cells were cultivated in DMEM and protein expression was induced for 14 h in DMEM 1% FCS. Cells were starved 3 h prior harvesting and ligand stimulation was performed 10 min before cell lysis, with PDGFAA and SCF (at 100 ng/ml) for PDGFR and KIT proteins, respectively. Figures are representative Western Blots from 3 biological replicates. Counter stains are provided as control. **a.** Signalling derived from stimulated KIT and PDGFRA WT receptors are compared to single point mutant KIT V559D signalling. Phosphorylation of PDGFR (Y849), KIT(Y703), PLCγ (Y783), STAT3 (Y705), MEK1/2 (Ser217/221), AKT (Ser473) and ERK1/2 (T202pY204) was monitored by Western blot analysis with the respective antibodies. **b and c.** Signalling from stimulated KIT and PDGFRA mutant receptors are compared. Phosphorylation of PDGFR (Y849), KIT(Y703), PLCγ (Y783), STAT1(Y701) , STAT3 (Y705), STAT5 (Y794), MEK1/2 (Ser217/221), AKT (Ser473) and ERK1/2 (T202pY204) was monitored by western blot analysis with the respective antibodies. **d.** Signalling from SCF stimulated GIST primary cell lines GIST48 and GIST882 for the indicated time points, after 6 h' starvation (0%FCS). Phosphorylation of KIT (Y703), AKT (Ser473) and ERK1/2 (T202pY204) was monitored by western blot analysis with the respective antibodies.
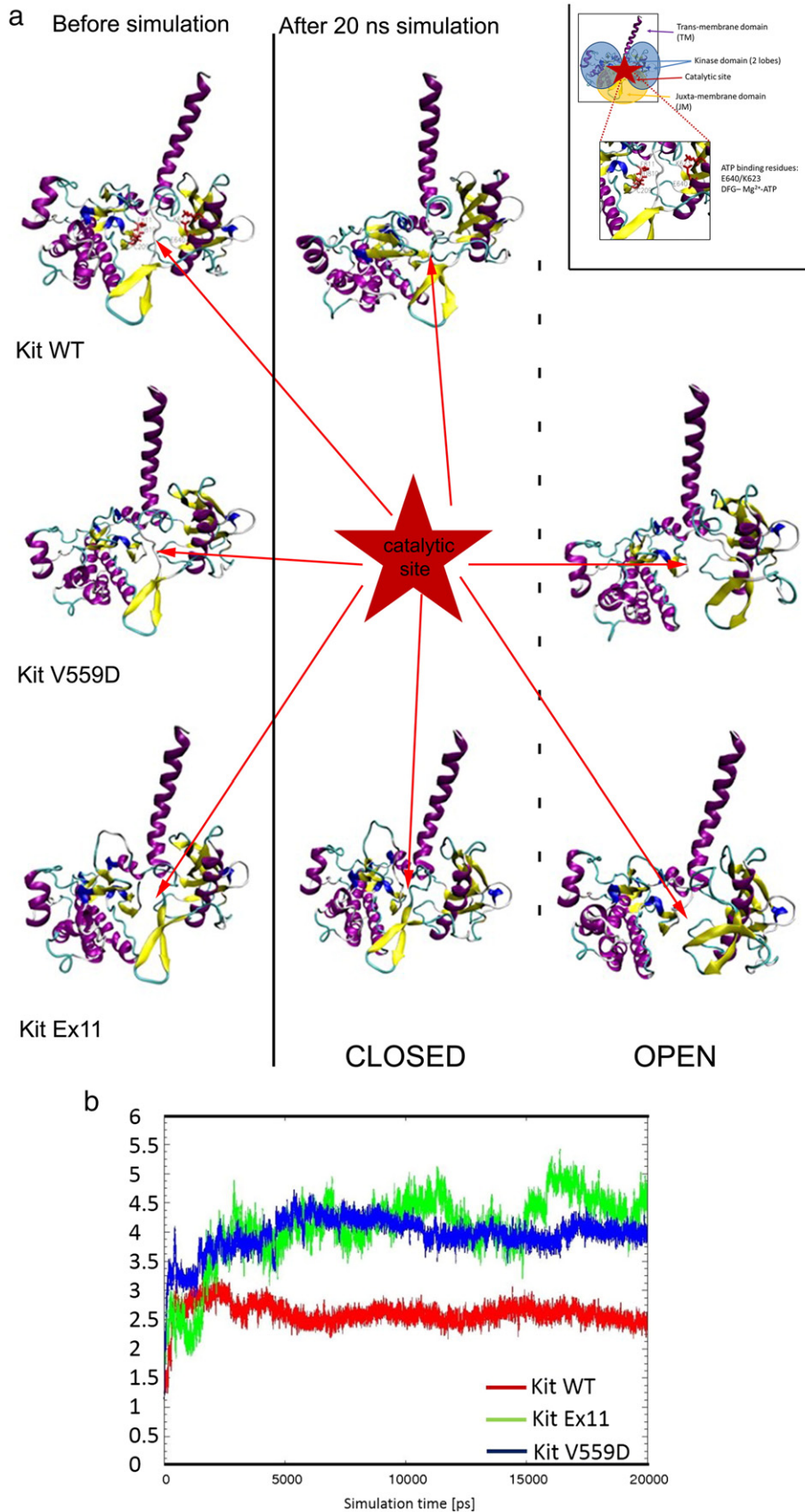
Fig. 3. Molecular dynamics simulation of KIT WT and KIT mutants. **a.** 3D structures of KIT WT and mutants before (left panels) and after stimulation (right panels). Important residues for ATP recognition are represented as red sticks and highlighted in the right insert at the top of the Figure. The two lobes of the kinase domain are schematically represented by blue circles and the Juxtamembrane domain by in yellow. Open and closed conformations derived from the ability of ATP molecules to enter (OPEN) or not (CLOSED) the catalytic site of the enzyme, as described previously [50] **b.** Backbone RMSD versus time plot during the 20 ns molecular dynamics simulation for KIT WT (red), KIT V559D (blue) and KIT Ex11 deletion mutant (green).

compartment. The single point mutant KIT V559D exhibited an overall weak KIT expression. Upon SCF addition, KIT WT is rapidly phosphorylated and degraded. The mutant proteins are constitutively phosphorylated and redirected to the cytosol after stimulation, where their degradation is less pronounced compared to the WT protein.

3.3. Signalling characteristics

Type III receptor tyrosine kinases conventionally activate MAPK and PI3K/Akt pathways upon ligand stimulation [3,24]. We compared the activation of these pathways before and after ligand stimulation between PDGFRA and KIT wild types to their respective GIST mutants. As indicated in Fig. 2a, the WT receptors are only phosphorylated upon addition of their respective ligands, which induces the downstream phosphorylation of key kinases for PI3K and MAPK pathways activation, namely Akt and Erk1/2. The introduction of the point mutation V559D in KIT initiates the expression of a constitutively phosphorylated protein, which exhibits a weak constitutive Akt and Erk1/2 phosphorylation. The induction of the conventional KIT regulated pathways is comparable to the wild type protein after SCF addition. Constitutive Akt activation was similar in intensity for all PDGFRA, KIT Ex9 and KIT Ex11 mutants (Fig. 2b). In contrast, the constitutive Erk1/2 activation was stronger for PDGFRA mutants, compared to KIT mutants. The MAPK/ERK activation required SCF stimulation to reach the activation level observed for PDGFRA mutants. PLCγ activation was found to be PDGFRA specific since neither KIT WT nor KIT mutants was able to induce the phosphorylation of PLCγ (Fig. 2c), regardless of the SCF stimulation. Another striking difference between KIT and PDGFRA WT stimulations resides in the kinetics of their activation (Fig. 3 in [11]). While the stimulation of PDGFRA by PDGFAA induces a sustained Akt and Erk activation for up to 48 h, stimulating KIT by SCF induces a rapid but transient (30–45 min) activation of these pathways. The activation of STAT (signal transducer and activator of transcription) was observed for none of the investigated time points, neither for PDGFRA nor for KIT WT proteins (STAT3 is shown as representative STAT factor in Fig. 2a). In contrast, the PDGFRA mutants were strong activators of the three investigated STAT species; namely STAT1, STAT3 and STAT5 (Fig. 2c and [13]). KIT Ex11 deletion mutant had an intermediate STATs activation capacity whereas KIT Ex9 mutant was identified as a weak STATs activator (Fig. 2c). We observed that ligand addition increased the activation of STAT species for KIT Ex9 mutant (Fig. 3 in [11]). However, nuclear translocation (Fig. 4a in [11]), required to obtain an efficient transcription factor activity, was exclusively detected for KIT Ex11 deletion mutant. This indicates its ability to elicit an efficient induction of STAT- dependent genes (Fig. 4b in [11]). Interestingly, the primary GIST cell line GIST48, exhibiting a homozygous mutation in KIT Ex 11, was also responsive to SCF stimulation (Fig. 2d). A weak response to SCF was noticed for GIST882 that harbors a KIT Ex13 homozygous mutation. A 1.5 to 2 fold increase in KIT and Akt phosphorylation occurs few minutes after stimulation. The reasons for the weak SCF stimulation observed for GIST882 could not be identified, however we may speculate that this is due to the higher endogenous expression of SCF measured in GIST882 relative to GIST48 (data not shown). Thus, GIST882 signalling may be already at its maximal intensity due to the endogenous SCF stimulation. Unfortunately, both cell lines did not tolerate a long term FCS starvation, impeding us to investigate the effect of SCF silencing on GIST cells proliferation (data not shown).

In conclusion, the point mutant V559D has a weak intrinsic kinase activity, more similar to KIT WT than to the other mutants, except for the constitutive phosphorylation of the receptor. The three PDGFRA mutants exhibit a quite strong intrinsic kinase activity regardless of ligand stimulation. The kinase activity of the KIT mutants is, qualitatively and quantitatively, more diverse. Only KIT Ex11 deletion mutant is an efficient STAT activator. The activation of Erk1/2 by KIT Ex9 is more transient when compared to KIT Ex11 deletion mutant, whereas the Akt activation was more sustained for all stimulated KIT mutants. More

importantly, all KIT mutants were responding to their natural ligand by an increase in PI3k/Akt and MAPK signalling intensities, including the primary cell line GIST48.

### 3.4. Molecular dynamics simulation

In order to elucidate the reasons for the differences in signalling capacities between the point mutant KIT V559D and the deletion mutant within the same exon, we built the respective 3D models starting from the crystal structures available for KIT WT protein (see Material and Methods part for model building details). The inhibitory loop formed by the juxtamembrane domain is released by the two types of mutation (Fig. 3a). This allows ATP molecules to reach the catalytic site located within the cleft separating the two lobes of the kinase, which justifies the constitutive phosphorylation of these receptors. We compared the ability of the two KIT Exon 11 mutants to accommodate ATP within the catalytic sites of the kinase. For that, the distance between the ATP binding residues, indicated as red sticks in Fig. 3a, was assessed. Glutamic acid 640 interacts with the side chain of Lysine 623, which forms a bridge with the ATP molecule while the DFG motif (D810-F811-G812) binds the ATP-linked Mg^{2+} ions [25]. The results of 20 ns molecular dynamic simulations are reported in Fig. 3b, showing that the deletion mutant is more flexible than the point mutant, which is in equilibrium between an open and a closed conformations. This could point towards a weaker stability of the point mutant V559D, enforced in a constant open and active conformation that is quickly degraded and recycled.

3.5. Impact of the different GIST mutations on global gene expression

Next we investigated the transcriptional changes induced by the different mutations using micro-array analyses comparing the global gene expression profiles of KIT WT, KIT Ex9 and KIT Ex11 deletion mutant after ligand stimulation. The background expression level was obtained from KIT WT without stimulation. Due to the weak signalling capacities of KIT V559D, this mutant was excluded from this analysis and gene expression levels were, when required, assessed by quantitative PCR. The global gene expression changes, derived from the PDGFRA mutants, were retrieved from our previous analysis [8]. We first compared the overall gene expression signature of KIT mutant and KIT WT by means of a rank-rank hypergeometric overlap (RRHO) analysis [16] allowing a comparison without the application of any cutoff. The genes lists were ranked according to their p-value and the significance of the overlap between the two lists was calculated while stepping through the two lists of genes (Fig. 4a). The similarity was highest between KIT Ex9 and KIT Ex11 mutants stimulated with SCF for 24 h. However, the similarity between these two KIT mutants is far from that observed previously between the three PDGFRA mutants [8]. The spearman correlation obtained for the PDGFRA mutants comparison was close to 0.7 against 0.3 for the KIT mutants.

In order to identify a common GIST signature, we compared the differentially expressed genes (DEG) common to KIT mutants (KIT Ex11 and KIT Ex9, both stimulated with SCF) and the previously proposed PDGFRA GIST mutants signature ([13] and Fig. 4b). We identified 140 genes, which were commonly de-regulated in all the investigated GIST mutants. Functional analysis of this GIST signature with KEGG pathway [26] reveals enrichment of "sprouty family members" and of "MAPK signalling pathway" related genes (Table 2). The regulation of SPROUTY family members, negative feedback regulators of RTKs, was validated by qPCR for all mutants (data not shown). Interestingly, SPRY4 was identified as a candidate for targeted therapy in GIST with oncogenic Kit mutation [27]. Thus, evaluatiing the expression level of other sprouty family members could be highly valuable for all non WT-GIST.

More than half of the Top25 GIST regulated genes (Table 3), including the sprouty family members, belong to MAPK pathway signalling. The transcription factor ETV1, recently described to promote
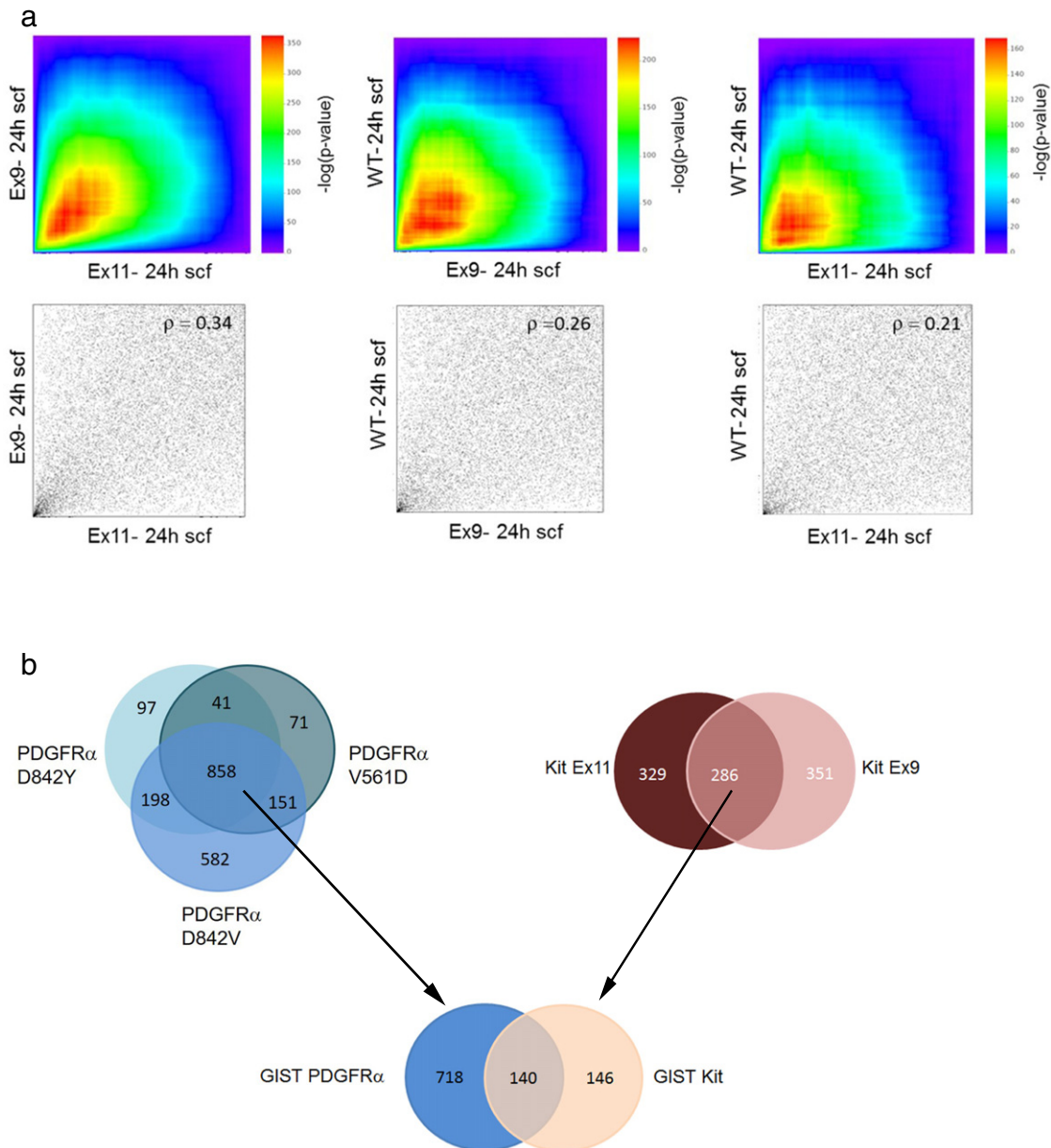
Fig. 4. Biological response of KIT mutant proteins differs greatly. **a.** RRHO heatmaps (upper row) and rank-rank scatter plots (lower row) for the comparison of stimulated KIT WT and oncogenic KIT proteins. The compared gene lists were ranked according to the ANOVA *p*-values attributed to the differentially expressed genes using non-stimulated KIT WT as control. The top differentially expressed genes are thus located at the lower left corner of the graph. For the heat maps, the range of -log10 - transformed hypergeometric *p*-values are indicated in the color scale bar. High intensity signals (red) indicate the highest overlap in the lists above the current sliding rank threshold (between the rank 1 for both lists at the bottom left corner and the colored point on the map). **b.** establishment of common GIST signature, including PDGFRA [8] and KIT DEGs. 114 genes are commonly regulated by all investigated GIST mutants.

tumorigenesis in GIST [28], was identified among them. Noteworthy all PEA3 family members, ETV1, ETV4 and ETV5, are highly up-regulated in all GIST mutants. The up-regulation of the MAPK pathway related genes is constitutive for all the mutants, but further increased for KIT EX9 and

KIT Ex11 mutants upon SCF stimulation (Fig. 5). Interestingly, some markers proposed for GIST diagnostic/prognostic were identified within the GIST signature (Table 4). The up-regulation of these potential GIST markers in our "*in vitro* model" implies that their regulation path is

Table 2
Functional classification for commonly regulated genes by all GIST mutants.

Term	Genes	Count	%	P-Value	FDR
SPROUTY family members	**SPRY2, IL12A, SPRED2, IL6R, SPRED1, SPRY4**	**6**	**4.3**	**1.20E-02**	**2.10E-01**
MAPK signalling pathway	**DUSP5, FOS, DUSP1, NR4A1, GADD45B, GADD45A, DDIT3, TGFB1**	**8**	**5.7**	**9.40E-03**	**2.40E-01**
Circadian rhythm	PER2, BHLHE40, CRY1	3	2.1	5.90E-03	2.90E-01
p53 signalling pathway	PMAIP1, GADD45B, SESN2, GADD45A	4	2.9	2.30E-02	2.90E-01

Table 3
Top 25 DEG common in PDGFRA and KIT mutants.

	Ratio KIT Ex11 deletion mutant with SCF vs KIT WT0	Ratio PDGFRA V561D vs PDGFRA WT0
EGR1	20.4	15.9
GPR50	17.9	11.2
ARC	6.4	6.7
FOSL1	6.2	3.0
GPR3	6.1	2.3
CHAC1	5.7	2.9
SERPINB2	5.6	6.0
TNFRSF12A	5.6	4.4
TFPI2	4.9	4.5
ETV4	4.9	2.0
ETV5	4.9	9.5
FOS	4.8	8.3
GADD45B	4.8	2.9
SPRED1	4.3	2.6
SESN2	4.2	2.6
EGR3	4.1	7.3
EPHA2	4.1	3.1
TGFB1	3.5	2.2
CSRNP1	3.5	3.0
ETV1	3.4	2.2
DDIT3	3.3	1.5
SPRY4	3.2	1.7
SPRY2	3.1	2.3
STC2	3.1	1.5
ZFP36	3.1	3.6
NAALAD2	0.6	0.6
KBTBD10	0.6	0.6

The genes that are down regulated in GIST primary cell lines when applying the MAPK pathway inhibitor PD0325901 are indicated in bold.

directly linked to the constitutive activation of the receptors and highlights their interest as GIST diagnostic markers. Remarkably, 4 out of 5 may be linked to MAPK pathway.

Since KIT Exon 11 deletion mutation is associated with poor outcome [29], we also investigated the KIT Ex11 specific gene signature, comparing KIT Exon 11 deletion mutant regulated genes to other GIST mutants (PDGFRA mutants and KIT Exon 9). 277 genes (Table 3 in [11]) were differentially expressed in KIT Ex11 deletion mutant only. Genes associated with "cell cycle" and "insulin signalling pathway" were found to be enriched by KEGG pathway analysis. The role of the genes specifically induced by the mutants Kit Ex 11 in GIST progression will be the subject of further investigation.

3.6. Effect of MAPK inhibitor on the proliferation of GIST primary cells

Since MAPK signalling axis was found to be a pillar in the GIST signature, we though to test the effect of MAPK inhibitor on GIST primary cell growth. For this purpose, we used a specific MEK inhibitor, PD0325901, already in clinical trials for different cancer types like NSCLC or CRC [30]. We first assessed the inhibitor specificity and dose response in two primary GIST cell lines, GIST48 and GIST882, imatinib resistant and sensitive, respectively. We found that, starting at 100 nM, PD0325901 specifically inhibits ERK1/2 phosphorylation without decreasing Akt, KIT or STATs activation (Fig. 6a). As assessed by western blot analysis, inhibition of ERK1/2 phosphorylation was already observed 1 h after the addition of the inhibitor and persisted for at least 30 h (data not shown). We then investigated the viability of the GIST primary cell lines after incubation with the MEK inhibitor at different concentrations and deduced the efficacy of the inhibitor for each cell line. The results (Fig. 6b for GIST882) indicate that PD0325901 decreases the cell viability of the imatinib sensitive cell line with an IC50 of around 80 nM. We could observe a further decrease in cell viability using the newly developed RTK inhibitor XL184 together with the MEK inhibitor PD0325901. Investigation of the synergistic potential between the two compounds using the CompuSyn software [31] reveals Combination Index (CI)

values below 1, indicating a positive synergy between the two compounds (Fig. 5 in [11]).

In conclusion, the MAPK pathway is a good target for GIST treatment and the combination of RTK and MAPK inhibitors could help preventing the emergence of RTK-inhibitor resistance.

4. Discussion

KIT mutant signalling has been extensively investigated but most results derived from GIST primary material [32,33], where patient specific features make a systematic comparison quite challenging. Additional knowledge resulted mainly from investigations on KIT D816V responsible for 90% of systemic mastocytosis [34,35]. To overcome the lack of knowledge related to PDGFRA mutants in GIST, we recently performed a thorough investigation of the 3 main PDGFRA mutants [8] found in GISTs. Interestingly, the three mutants exhibited very similar signalling properties that differ from the PDGFRA WT protein. We thereofore extended the comparison to PDGFRA and main KIT mutants detected in GIST.

We found striking differences in protein localization and in intrinsic kinase activities between the three investigated KIT mutants. In line with a recent study where KIT V560D exhibited a weaker kinase activity compared to the systemic mastocytosis mutant KIT D816V [36], the point mutant KIT V559D displayed a weak intrinsic kinase activity compared to Kit Ex9 or Kit Ex11 mutants. Interestingly enough, the Ex11 deletion mutation is at the same time associated with a high risk factor [29, 37,38] and known to be a good responder to imatinib treatment [39]. In the present study we propose some insights into this apparent contradiction. First, comparing the structures of two KIT Ex11 mutants using molecular dynamics simulation, we found that KIT Ex11 deletion mutant exhibited a high flexibility between an open and a closed conformation. In contrast, Kit V559D was less flexible and locked in a closed conformation. The high flexibility observed in KIT Ex11 deletion mutant might allow imatinib to be particularly efficient in patients carrying KIT Ex11 deletion mutation. Second, we found KIT V559D unable to efficiently activate the STAT transcription factors. We conclude that the intracellular retention in the ER/Golgi compartment observed for KIT V559D mutant is required, as previously observed for PDGFRA mutants [8], but not sufficient to achieve a good activation of the STAT species by RTKs. In addition, Kit Ex11 deletion mutant exhibits the highest intrinsic kinase activity compared to the other KIT mutants and was the only mutant able to elicit an efficient STATs activation. The role and activation status of STAT species in GIST remains largely unknown. Duensing et al. [33] investigated the STATs activation profiles of 15 patients, giving a quite heterogeneous picture. No STAT5 activation could be detected in patient samples. STAT5 phosphorylation was indeed the most unstable and difficult to observe in GIST primary cell lines: GIST882 and GIST48. STAT3 was activated in almost all patients and STAT1 activation was found higher in Exon 11 missense mutants compared to Ex11 deletion mutants [33]. We could demonstrate here that activation of STATs is part of the KIT Ex11 deletion kinase activity and could be initiated by Kit Ex9 mutant after SCF stimulation. The role of the STAT factors in GIST initiation and progression remains intriguing and deserves further investigations.

In the continuous efforts to identify new targets for GIST patients, PI3K [40,41] or Hsp90 inhibitors [42,43] were anticipated as promising for the treatment of imatinib-resistant GIST but no FDA approval has been delivered so far. In the present study, we showed that MAPK activation was the most prominent pathway commonly induced by all studied GIST mutants at the transcriptional level. Interestingly, not only ETV1 was up-regulated in all GIST mutants, but also the other members of the PEA3 family, ETV4 and ETV5. ETV1 was recently identified as a key transcription factor for GIST development [28,44] and it appears now mandatory to consider the role of ETV4 and ETV5 in GIST initiation and progression. Upon imatinib treatment, MAPK-induced genes are rapidly but only transiently down-regulated in imatinib
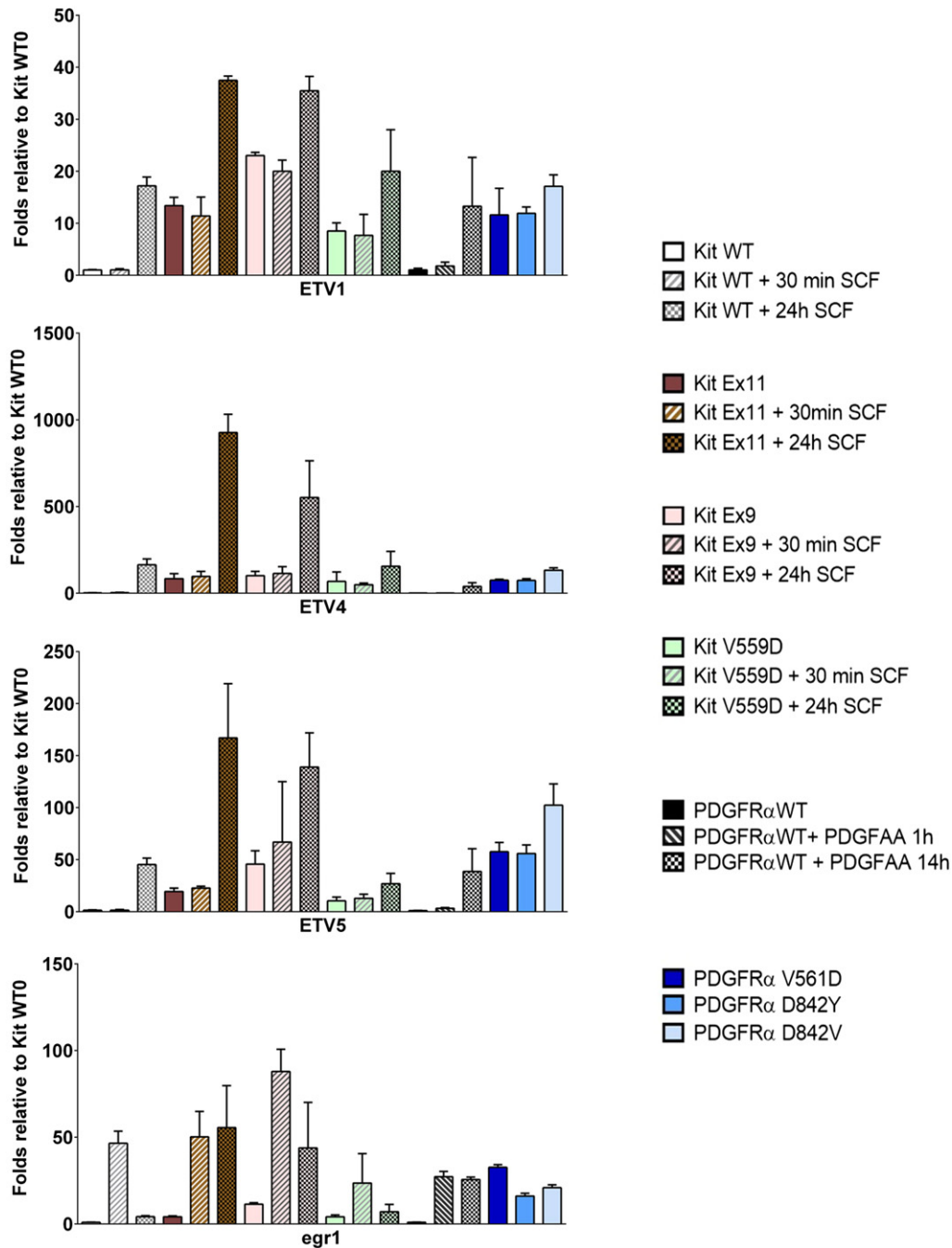
Fig. 5. Up-regulation of MAPK pathway downstream genes by PDGFRA and Kit mutants. mRNA expression level of ETV1, ETV4, ETV5 and egr1 in KIT and PDGFRA WT and mutants. Protein expression was induced by 5 ng/ml doxycycline for 24 h, cells were starved 3 h before harvesting. KIT expressing cells were stimulated with 100 ng/ml SCF for either 30 min or 24 h. PDGFRA WT expressing cells were stimulated with 100 ng/ml PDGFAA for either 30 min or 14 h. $n = 3$, Mean $\pm$ SD.

Table 4
Potential GIST markers confirmed by our study to be KIT and PDGFRA dependent.

Marker/ possible targets in GIST	Reference	Gene identified by the present work
Actin	[51]	ACTBL2
Sonic hedgehog pathway	[52]	HHIP, KDM6B
ETV1	[53,54]	ETV1, ETV4, ETV5
KCTD10 (ubiquitin-protein transferase activity)	[55]	KCTD12, KCTD13
RBPMS2	[56]	RBPMS2
Spry4	[27]	SPRY4, SPRY2, SPRED1, SPRED2

sensitive cells (Fig. 6 in [11]). A recent study [45] proposed that a FGFR-mediated reactivation of the MAPK pathway was responsible for the transient character of imatinib treatment. Therefore, combining imatinib and MAPK inhibition could reduce the MAPK reactivation and decrease the risks of developing resistance. A clinical trial phase Ib/II is currently testing the efficiency of such a combination using MEK162 together with imatinib (NCT01991379) [44]. We identified PD0325901 as a very efficient MEK inhibitor, able to abolish MAPK activation starting a concentration of 100 nM in both imatinib resistant and sensitive GIST cells for a long period of time, which is not achieved by imatinib alone. Our data support the development of combination therapy to treat
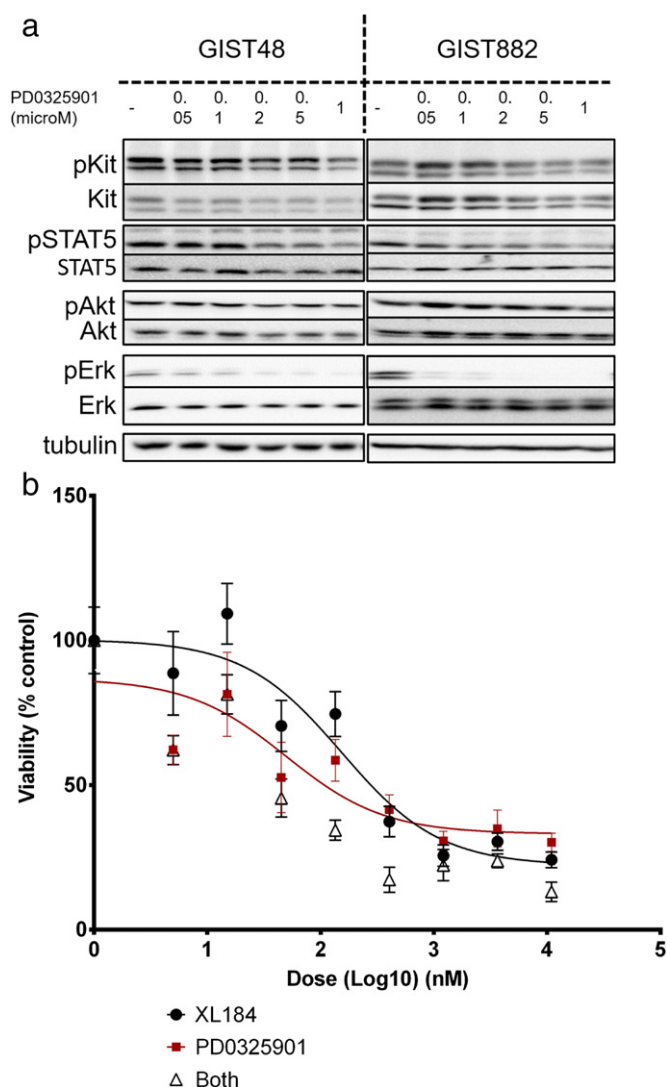
Fig. 6. Inhibition of MAPK signalling by PD0325901 in GIST primary cell lines. **a.** Western blot analysis indicating the phosphorylation status of KIT, STAT5, Akt and Erk in GIST primary cell lines GIST882 and GIST48 after treatment with MEK inhibitor PD0325901 at different concentrations. **b.** GIST882 viability as determined by PrestoBlue after treatment with various doses of RTK inhibitor (XL-184) and MEK inhibitor (PD0325901) or both of them simultaneously for 30 h. Representative data of 3 biological replicates. Each point represents the mean of a technical duplicate.

GIST patients and overcome the development of RTK inhibitor resistance.

Finally, the major difference between PDGFRA and KIT mutants identified in the present study is the ligand-driven activation demonstrated by all KIT mutants expressed in an isogenic background. While PDGFRA mutants proffered a maximal constitutive kinase activity without possible stimulation by their ligand PDGFAA, KIT mutants remained responsive to their natural ligand, SCF. The capacity of KIT mutants to be further stimulated by their natural ligand SCF was confirmed in GIST48, which is a GIST primary cell line with homozygous mutation in KIT Ex11. SCF activation of GIST primary cell lines was recently identified [46,47] and authors could demonstrate an increased proliferation upon SCF stimulation, which was associated with the heterozygous nature of the mutations found in these patients [46,47]. With the present investigation, we could in fact demonstrate that KIT mutants, at least KIT Ex9 and KIT Ex11 mutants, may be stimulated by KIT ligand SCF. This previously unknown feature of KIT mutants is of great importance in the context of GIST since stem cell factor expression was found

positive in 76% of patient samples and was associated with high risk [46–49]. The maximal signalling capacities of KIT mutants were only achieved upon SCF stimulation and this should be considered in future investigations. It remains unclear how the constitutive signalling of the mutants is increased by SCF or how/whether the receptor trafficking is involved in this process. This should be investigated in more details in the future, including the stoichiometry of the different mutant proteins both in presence and absence of ligand. In any case, SCF plays a major role in the signalling properties of KIT mutants and its expression level in patients could be helpful for prognostic purposes. In the same line, the possibility to target SCF using antibodies should be considered in the future.

5. Conclusion

The importance of the nature of the mutations in GIST has been previously identified and efficiently used for diagnostic and therapeutic purposes. We now demonstrate that constitutively active KIT mutants retained the ability to be further stimulated by their natural ligand. This is of high importance for the signalling properties of the kinases and should be carefully considered in future studies investigating alternative therapeutic agents. We also propose the specific MEK inhibitor PD0325901 as a promising drug in combination with Imatinib.

Competing interests

The authors declare that they have no conflicts of interest.

Acknowledgments

Abbreviations

GIST	gastro-intestinal stromal tumors
PDGFR	Platelet-derived growth factor receptor
PDGFAA	Platelet-derived growth factor AA
SCF	stem cell factor
MAPK	Mitogen-activated protein kinases
ERK1/2	Extracellular signal-regulated kinases
RTK	receptor tyrosine kinase

References

[1] C.L. Corless, J.A. Fletcher, M.C. Heinrich, Biology of gastrointestinal stromal tumors, J. Clin. Oncol. 22 (18) (2004) 3813–3825.

[2] H. Yamamoto, Y. Oda, K. Kawaguchi, N. Nakamura, T. Takahira, S. Tamiya, T. Saito, Y. Oshiro, M. Ohta, T. Yao, M. Tsuneyoshi, c-kit and PDGFRA mutations in extragastrointestinal stromal tumor (gastrointestinal stromal tumor of the soft tissue), Am. J. Surg. Pathol. 28 (4) (2004) 479–488.

[3] L. Rönnstrand, Signal transduction via the stem cell factor receptor/c-Kit, Cell. Mol. Life Sci. 61 (19–20) (2004) 2535–2548.

[4] R. Robert Jr., Structure and regulation of Kit protein-tyrosine kinase—The stem cell factor receptor, Biochem. Biophys. Res. Commun. 338 (3) (2005) 1307–1315.

[5] P.G. Casali, J.Y. Blay, A. Bertuzzi, S. Bielack, B. Bjerkehagen, S. Bonvalot, I. Boukovinas, P. Bruzzi, A.P.D. Tos, P. Dileo, M. Eriksson, A. Fedenko, A. Ferrari, S. Ferrari, H. Gelderblom, R. Grimer, A. Gronchi, R. Haas, K.S. Hall, P. Hohenberger, R. Issels, H. Joensuu, I. Judson, A. Le Cesne, S. Litiere, J. Martin-Broto, O. Merimsky, M. Montemurro, C. Morosi, P. Picci, I. Ray-Coquard, P. Reichardt, P. Rutkowski, M. Schlemmer, S. Stacchiotti, V. Torri, A. Trama, F. Van Coevorden, W. Van der Graaf, D. Vanel, E. Wardelmann, E.E. Sarcoma, Gastrointestinal stromal tumours: ESMO Clinical Practice Guidelines for diagnosis, treatment and follow-up, Ann. Oncol. 25 (2014) 21–26.

[6] R.P. Dematteo, K.V. Ballman, C.R. Antonescu, R.G. Maki, P.W. Pisters, G.D. Demetri, M.E. Blackstein, C.D. Blanke, M. von Mehren, M.F. Brennan, S. Patel, M.D. McCarter, J.A. Polikoff, B.R. Tan, K. Owzar, A.C.o.S.O.G.A.I.A.G.S. Team, Adjuvant imatinib mesylate after resection of localised, primary gastrointestinal stromal tumour: a

randomised, double-blind, placebo-controlled trial, Lancet 373 (9669) (2009) 1097–1104.

[7] J. Verweij, P.G. Casali, J. Zalcberg, A. LeCesne, P. Reichardt, J.Y. Blay, R. Issels, A. van Oosterom, P.C.W. Hogendoorn, M. Van Glabbeke, R. Bertulli, I. Judson, E.S.T.B.S. Grp, G. Italian Sarcoma, T. Australasian Gastrointestinal, Progression-free survival in gastrointestinal stromal tumours with high-dose imatinib: randomised trial, Lancet 364 (9440) (2004) 1127–1134.

[8] C. Bahlawane, R. Eulenfeld, M.Y. Wiesinger, J. Wang, A. Muller, A. Girod, P.V. Nazarov, K. Felsch, L. Vallar, T. Sauter, V.P. Satagopam, S. Haan, Constitutive activation of oncogenic PDGFR alpha-mutant proteins occurring in GIST patients induces receptor mislocalisation and alters PDGFR alpha signalling characteristics, Cell Commun. Signal 13 (2015).

[9] D.A. Tuveson, N.A. Willis, T. Jacks, J.D. Griffin, S. Singer, C.D. Fletcher, J.A. Fletcher, G.D. Demetri, STI571 inactivation of the gastrointestinal stromal tumor c-KIT oncoprotein: biological and clinical implications, Oncogene 20 (36) (2001) 5054–5058.

[10] R. Halaban, M. Krauthammer, M. Pelizzola, E. Cheng, D. Kovacs, M. Sznol, S. Ariyan, D. Narayan, A. Bacchiocchi, A. Molinaro, Y. Kluger, M. Deng, N. Tran, W. Zhang, M. Picardo, J.J. Enghild, Integrative analysis of epigenetic modulation in melanoma cell response to decitabine: clinical implications, PLoS One 4 (2) (2009) e4563.

[11] C. Bahlawane, M. Schmitz, E. Letellier, K. Arumugam, N. Nicot, P.V. Nazarov, S. Haan, Data on Insights into ligand stimulation effects on gastro-intestinal stromal tumors signalling Data in Brief (submitted).

[12] C. Haan, I. Behrmann, A cost effective non-commercial ECL-solution for Western blot detections yielding strong signals and low background, J. Immunol. Methods 318 (1–2) (2007) 11–19.

[13] C. Bahlawane, R. Eulenfeld, M.Y. Wiesinger, J. Wang, A. Muller, A. Girod, P.V. Nazarov, K. Felsch, L. Vallar, T. Sauter, V.P. Satagopam, S. Haan, Constitutive activation of oncogenic PDGFR alpha-mutant proteins occurring in GIST patients induces receptor mislocalisation and alters PDGFR alpha signalling characteristics, Cell Commun. Signal 13 (2015) 21.

[14] S. Haan, C. Bahlawane, J. Wang, P.V. Nazarov, A. Muller, R. Eulenfeld, C. Haan, C. Rolvering, L. Vallar, V.P. Satagopam, T. Sauter, M.Y. Wiesinger, The oncogenic FIP1L1-PDGFRalpha fusion protein displays skewed signaling properties compared to its wild-type PDGFRalpha counterpart, Jak-Stat 4 (1) (2015) e1062596.

[15] M.E. Ritchie, B. Phipson, D. Wu, Y. Hu, C.W. Law, W. Shi, G.K. Smyth, limma powers differential expression analyses for RNA-sequencing and microarray studies, Nucleic Acids Res. 43 (7) (2015).

[16] S.B. Plaisier, R. Taschereau, J.A. Wong, T.G. Graeber, Rank-rank hypergeometric overlap: identification of statistically significant overlap between gene-expression signatures, Nucleic Acids Res. 38 (17) (2010), e169.

[17] S.A. Bustin, V. Benes, J.A. Garson, J. Hellemans, J. Huggett, M. Kubista, R. Mueller, T. Nolan, M.W. Pfaffl, G.L. Shipley, J. Vandesompele, C.T. Wittwer, The MIQE Guidelines: Minimum Information for Publication of Quantitative Real-Time PCR Experiments, Clin. Chem. 55 (4) (2009) 611–622.

[18] J. Hellemans, J. Vandesompele, Selection of reliable reference genes for RT-qPCR analysis, Methods Mol. Biol. 1160 (2014) 19–26.

[19] S. Bamford, E. Dawson, S. Forbes, J. Clements, R. Pettett, A. Dogan, A. Flanagan, J. Teague, P.A. Futreal, M.R. Stratton, R. Wooster, The COSMIC (Catalogue of Somatic Mutations in Cancer) database and website, Br. J. Cancer 91 (2) (2004) 355–358.

[20] F. Haller, N. Happel, H.-J. Schulten, A. von Heydebreck, S. Schwager, T. Armbrust, C. Langer, B. Gunawan, D. Doenecke, L. Fuzesi, Site-dependent differential KIT and PDGFRA expression in gastric and intestinal gastrointestinal stromal tumors, Mod. Pathol. Off. J. U. S. Can. Acad. Pathol. Inc 20 (10) (2007) 1103–1111.

[21] C.L. Corless, L. McGreevey, A. Haley, A. Town, M.C. Heinrich, KIT mutations are common in incidental gastrointestinal stromal tumors one centimeter or less in size, Am. J. Pathol. 160 (5) (2002) 1567–1572.

[22] M.C. Heinrich, C.L. Corless, G.D. Demetri, C.D. Blanke, M. von Mehren, H. Joensuu, L.S. McGreevey, C.J. Chen, A.D. Van den Abbeele, B.J. Druker, B. Kiese, B. Eisenberg, P.J. Roberts, S. Singer, C.D. Fletcher, S. Silberman, S. Dimitrijevic, J.A. Fletcher, Kinase mutations and imatinib response in patients with metastatic gastrointestinal stromal tumor, J. Clin. Oncol. 21 (23) (2003) 4342–4349.

[23] S. Brahimi-Adouane, J.B. Bachet, S. Tabone-Eglinger, F. Subra, C. Capron, J.Y. Blay, J.F. Emile, Effects of endoplasmic reticulum stressors on maturation and signaling of hemizygous and heterozygous wild-type and mutant forms of KIT, Mol. Oncol. 7 (3) (2013) 323–333.

[24] J. Lennartsson, T. Jelacic, D. Linnekin, R. Shivakrupa, Normal and oncogenic forms of the receptor tyrosine kinase kit, Stem Cells 23 (1) (2005) 16–43.

[25] C. Mol, K. Lim, V. Sridhar, H. Zou, E. Chien, B. Sang, J. Nowakowski, D. Kassel, C. Cronin, D. McRee, Structure of a c-Kit product complex reveals the basis for kinase transactivation, J. Biol. Chem. 278 (34) (2003) 31461–31464.

[26] d.W. Huang, B.T. Sherman, R.A. Lempicki, Systematic and integrative analysis of large gene lists using DAVID bioinformatics resources, Nat. Protoc. 4 (1) (2009) 44–57.

[27] P. Gromova, S. Ralea, A. Lefort, F. Libert, B.P. Rubin, C. Erneux, J.-M. Vanderwinden, Kit K641E oncogene up-regulates Sprouty homolog 4 and Trophoblast glycoprotein in interstitial cells of Cajal in a murine model of gastrointestinal stromal tumours, J. Cell. Mol. Med. 13 (8A) (2009) 1536–1548.

[28] P. Chi, Y. Chen, L. Zhang, X. Guo, J. Wongvipat, T. Shamu, J.A. Fletcher, S. Dewell, R.G. Maki, D. Zheng, C.R. Antonescu, C.D. Allis, C.L. Sawyers, ETV1 is a lineage survival factor that cooperates with KIT in gastrointestinal stromal tumours, Nature 467 (7317) (2010) 849–853.

[29] J.B. Bachet, I. Hostein, A. Le Cesne, S. Brahimi, A. Beauchet, S. Tabone-Eglinger, F. Subra, B. Bui, F. Duffaud, P. Terrier, J.M. Coindre, J.Y. Blay, J.F. Emile, Prognosis and predictive value of KIT exon 11 deletion in GISTs, Br. J. Cancer 101 (1) (2009) 7–11.

[30] <ClinicalTrials.Gov>).

[31] T.-C. Chou, Drug Combination Studies and Their Synergy Quantification Using the Chou-Talalay Method, Cancer Res. 70 (2) (2010) 440–446.

[32] A. Duensing, M.C. Heinrich, C.D. Fletcher, J.A. Fletcher, Biology of gastrointestinal stromal tumors: KIT mutations and beyond, Cancer Investig. 22 (1) (2004) 106–116.

[33] A. Duensing, F. Medeiros, B. McConarty, N.E. Joseph, D. Panigrahy, S. Singer, C.D. Fletcher, G.D. Demetri, J.A. Fletcher, Mechanisms of oncogenic KIT signal transduction in primary gastrointestinal stromal tumors (GISTs), Oncogene 23 (22) (2004) 3999–4006.

[34] J.B. Bachet, S. Tabone-Eglinger, S. Dessaux, A. Besse, S. Brahimi-Adouane, J.F. Emile, J.Y. Blay, L. Alberti, Gene expression patterns of hemizygous and heterozygous KIT mutations suggest distinct oncogenic pathways: a study in NIH3T3 cell lines and GIST samples, PLoS One 8 (4) (2013), e61103.

[35] K. Hashimoto, I. Matsumura, T. Tsujimura, D.K. Kim, H. Ogihara, H. Ikeda, S. Ueda, M. Mizuki, H. Sugahara, H. Shibayama, Y. Kitamura, Y. Kanakura, Necessity of tyrosine 719 and phosphatidylinositol 3'-kinase-mediated signal pathway in constitutive activation and oncogenic potential of c-kit receptor tyrosine kinase with the Asp814Val mutation, Blood 101 (3) (2003) 1094–1102.

[36] O. Lindblad, J.U. Kazi, L. Rönnstrand, J. Sun, PI3 kinase is indispensable for oncogenic transformation by the V560D mutant of c-Kit in a kinase-independent manner, Cell. Mol. Life Sci. 72 (22) (2015) 4399–4407.

[37] A. Lv, Z. Li, X. Tian, X. Guan, M. Zhao, B. Dong, C. Hao, SKP2 High Expression, KIT Exon 11 Deletions, and Gastrointestinal Bleeding as Predictors of Poor Prognosis in Primary Gastrointestinal Stromal Tumors, PLoS One 8 (5) (2013).

[38] M.R. Cerski, F. Pereira, U.S. Matte, F.H. Oliveira, F.L. Crusius, L.E. Waengertner, A. Osvaldt, F. Fornari, L. Meurer, Exon 11 mutations, Ki67, and p16(INK4A) as predictors of prognosis in patients with GIST, Pathol. Res. Pract. 207 (11) (2011) 701–706.

[39] M. Debiec-Rychter, H. Dumez, I. Judson, B. Wasag, J. Verweij, M. Brown, S. Dimitrijevic, R. Sciot, M. Stul, H. Vranck, M. Scurr, A. Hagemeijer, M. van Glabbeke, A.T. van Oosterom, E.S.T.a.B.S. Group, Use of c-KIT/PDGFRA mutational analysis to predict the clinical response to imatinib in patients with advanced gastrointestinal stromal tumours entered on phase I and II studies of the EORTC Soft Tissue and Bone Sarcoma Group, Eur. J. Cancer 40 (5) (2004) 689–695.

[40] S. Bauer, A. Duensing, G.D. Demetri, J.A. Fletcher, KIT oncogenic signaling mechanisms in imatinib-resistant gastrointestinal stromal tumor: PI3-kinase/AKT is a crucial survival pathway, Oncogene 26 (54) (2007) 7560–7568.

[41] M.A. Pantaleo, G. Nicoletti, C. Nanni, C. Gnocchi, L. Landuzzi, C. Quarta, S. Boschi, M. Nannini, M. Di Battista, P. Castellucci, S. Fanti, P.L. Lollini, E. Bellan, M. Castelli, D. Rubello, G. Biasco, Preclinical evaluation of KIT/PDGFRA and mTOR inhibitors in gastrointestinal stromal tumours using small animal FDG PET, J. Exp. Clin. Cancer Res. 29 (2010) 173.

[42] W. Ying, Z. Du, L. Sun, K.P. Foley, D.A. Proia, R.K. Blackman, D. Zhou, T. Inoue, N. Tatsuta, J. Sang, S. Ye, J. Acquaviva, L.S. Ogawa, Y. Wada, J. Barsoum, K. Koya, Ganetespib, a unique triazolone-containing Hsp90 inhibitor, exhibits potent antitumor activity and a superior safety profile for cancer therapy, Mol. Cancer Ther. 11 (2) (2012) 475–484.

[43] T.Y. Lin, M. Bear, Z. Du, K.P. Foley, W. Ying, J. Barsoum, C. London, The novel HSP90 inhibitor STA-9090 exhibits activity against Kit-dependent and -independent malignant mast cell tumors, Exp. Hematol. 36 (10) (2008) 1266–1277.

[44] L. Ran, I. Sirota, Z. Cao, D. Murphy, Y. Chen, S. Shukla, Y. Xie, M.C. Kaufmann, D. Gao, S. Zhu, F. Rossi, J. Wongvipat, T. Taguchi, W.D. Tap, I.K. Mellinghoff, P. Besmer, C.R. Antonescu, Y. Chen, P. Chi, Combined Inhibition of MAP Kinase and KIT Signaling Synergistically Destabilizes ETV1 and Suppresses GIST Tumor Growth, Cancer Discov. 5 (3) (2015) 304–315.

[45] F. Li, H. Huynh, X. Li, D.A. Ruddy, Y. Wang, R. Ong, P. Chow, S. Qiu, A. Tam, D.P. Rakiec, R. Schlegel, J.E. Monahan, A. Huang, FGFR-Mediated Reactivation of MAPK Signaling Attenuates Antitumor Effects of Imatinib in Gastrointestinal Stromal Tumors, Cancer Discov. 5 (4) (2015) 438–451.

[46] C.-G. Bai, X.-W. Hou, F. Wang, C. Qiu, Y. Zhu, L. Huang, J. Zhao, J.-J. Xu, D.-L. Ma, Stem cell factor-mediated wild-type KIT receptor activation is critical for gastrointestinal stromal tumor cell growth, World J. Gastroenterol. 18 (23) (2012) 2929–2937.

[47] X.-W. Hou, C.-G. Bai, X.-H. Liu, C. Qiu, L. Huang, J.-J. Xu, D.-L. Ma, Expression of stem cell factor in gastrointestinal stromal tumors: Implications for proliferation and imatinib resistance, Oncol. Lett. 5 (2) (2013) 552–558.

[48] C. Qiu, X. Liu, C. Bai, D.L. Ma, The expression of KIT receptor dimers in gastrointestinal stromal tumors independent of c-kit mutation and SCF expression is associated with high-risk stratification, Oncol. Lett. 4 (4) (2012) 805–811.

[49] N. Théou-Anton, S. Tabone, D. Brouty-Boyé, R. Saffroy, L. Ronnstrand, A. Lemoine, J.F. Emile, Co expression of SCF and KIT in gastrointestinal stromal tumours (GISTs) suggests an autocrine/paracrine mechanism, Br. J. Cancer 94 (8) (2006) 1180–1185.

[50] C.D. Mol, D.R. Dougan, T.R. Schneider, R.J. Skene, M.L. Kraus, D.N. Scheibe, G.P. Snell, H. Zou, B.C. Sang, K.P. Wilson, Structural basis for the autoinhibition and STI-571 inhibition of c-Kit tyrosine kinase, J. Biol. Chem. 279 (30) (2004) 31655–31663.

[51] J. Ruiz-Tovar, M. Diez-Tabernilla, G. Housari, E. Martinez-Molina, A. Sanjuanbenito, Gastrointestinal Stromal Tumors: Actin Expression, a New Prognostic Factor? Am. Surg. 76 (11) (2010) 1244–1250.

[52] A. Yoshizaki, T. Nakayama, S. Naito, C.-Y. Wen, I. Sekine, Expressions of sonic hedgehog, patched, smoothened and Gli-1 in human intestinal stromal tumors and their correlation with prognosis, World J. Gastroenterol. 12 (35) (2006) 5687–5691.

[53] P. Birner, A. Beer, U. Vinatzer, S. Stary, R. Höftberger, N. Nirtl, F. Wrba, B. Streubel, S.F. Schoppmann, MAPKAP kinase 2 overexpression influences prognosis in gastrointestinal stromal tumors and associates with copy number variations on chromosome 1 and expression of p38 MAP kinase and ETV1, Clin. Cancer Res. 18 (7) (2012) 1879–1887.

[54] P. Chi, Y. Chen, L. Zhang, X. Guo, J. Wongvipat, T. Shamu, J.A. Fletcher, S. Dewell, R.G. Maki, D. Zheng, C.R. Antonescu, C.D. Allis, C.L. Sawyers, ETV1 is a lineage survival

factor that cooperates with KIT in gastrointestinal stromal tumours, Nature 467 (7317) (2010) (849-U117).

[55] D. Kubota, A. Yoshida, H. Tsuda, Y. Suehara, T. Okubo, T. Saito, H. Orita, K. Sato, T. Taguchi, T. Yao, K. Kaneko, H. Katai, A. Kawai, T. Kondo, Gene Expression Network Analysis of ETV1 Reveals KCTD10 as a Novel Prognostic Biomarker in Gastrointestinal Stromal Tumor, PLoS One 8 (8) (2013), e73896.

[56] I. Hapkova, J. Skarda, C. Rouleau, A. Thys, C. Notarnicola, M. Janikova, F. Bernex, M. Rypka, J.M. Vanderwinden, S. Faure, J. Vesely, P. de Santa Barbara, High expression of the RNA-binding protein RBPMS2 in gastrointestinal stromal tumors, Exp. Mol. Pathol. 94 (2) (2013) 314–321.